

Generative and Contrastive Self-Supervised Learning for Graph Anomaly Detection

Yu Zheng, Ming Jin, Yixin Liu, Lianhua Chi, Khoa T. Phan, Yi-Ping Phoebe Chen

Abstract—Anomaly detection from graph data has drawn much attention due to its practical significance in many critical applications including cybersecurity, finance, and social networks. Existing data mining and machine learning methods are either shallow methods that could not effectively capture the complex interdependency of graph data or graph autoencoder methods that could not fully exploit the contextual information as supervision signals for effective anomaly detection. To overcome these challenges, in this paper, we propose a novel method, Self-Supervised Learning for Graph Anomaly Detection (SL-GAD). Our method constructs different contextual subgraphs (views) based on a target node and employs two modules, *generative attribute regression* and *multi-view contrastive learning* for anomaly detection. While the *generative attribute regression* module allows us to capture the anomalies in the attribute space, the *multi-view contrastive learning* module can exploit richer structure information from multiple subgraphs, thus abling to capture the anomalies in the structure space, mixing of structure, and attribute information. We conduct extensive experiments on six benchmark datasets and the results demonstrate that our method outperforms state-of-the-art methods by a large margin.

Index Terms—Anomaly detection, self-supervised learning, graph neural networks (GNNs), unsupervised learning.

1 INTRODUCTION

RECENT years have witnessed increasing domains that continuously generate complex, interdependent, and connected data, represented in the form of graphs or networks. Typical examples include social networks, biological networks, traffic networks, and financial transaction networks, to name a few. Data mining and analysis from these graph-structured data have drawn much attention, particularly for the task of graph anomaly detection, where the goal is to identify patterns (e.g., nodes, edges, subgraphs) which differ significantly from the majority patterns in the graphs. For instance, in the financial transaction network, it is critically important to identify the abnormal edges (fraudulent transactions) between two accounts [1]. In a social network, it is also crucial to detect the abnormal nodes (social bots) as they may spread rumours over social networks [2].

Detecting graph anomalies however is a challenging task because many graphs contain complex linkage (structure) information as well as node attribute information. As a result, anomalies can be hidden in the structure space, attribute space, and the mix of both. Furthermore, in many cases, the ground truths of the anomalies are unknown, rendering many supervised classification approaches not applicable. These two challenges have motivated increasing efforts for efficient anomaly detection in recent years, ranging from shallow methods to deep representation methods for anomaly detection, in a purely unsupervised manner.

The shallow methods mainly focus on defining anomaly quantify measures for graphs and developing methods to capture the anomaly based on these measures. Perozzi and Akoglu [3] propose a normality measure to evaluate neighbourhoods both internally and externally by considering both attributes and graph structure, where Anomaly Mining of Entity Neighborhoods (AMEN) is proposed to optimise the measure to get the anomaly score. Noticing that the residual of regression plays an important role for qualifying the anomaly score, Li *et al.* [4] propose a Radar framework that learns a linear regression function to fit the node attributes regularized by the network structure. The residual from the regression function is used as a score to measure the anomaly. Similarly, Peng *et al.* [5] propose a joint modelling approach to conduct attribute selection and anomaly detection using the residual. While being simple, these shallows are not able to model (or capture) the complex interdependent relations of graphs.

Deep learning-based approaches have shown impressive progress in many domains, including image, text, and graphs. For the task of graph anomaly detection, autoencoder becomes a popular choice as it is a purely unsupervised framework and fits settings where no ground-truth label is available. Specifically, Dominant [6] employs a graph convolution network (GCN) to encode both structure and node content into a latent embedding, based on which both attribute and structure reconstruction decoders are used. The anomaly score is calculated by the weighted sum of the reconstruction errors of attribute and structure. SpaceAE [7] employs a spectral autoencoder with a density estimation model for anomaly detection. AEGIS [8] further generalises the graph autoencoder to the inductive setting where unseen anomalies may exist.

However, existing graph autoencoder based methods do not fully exploit the *contextual information* (e.g., neighbouring nodes or subgraphs) which is critically important for

- Y. Zheng, L. Chi, K. T. Phan, and Y-P. P. Chen are with Department of Computer Science and Information Technology, La Trobe University, Melbourne Australia
E-mail: Yu.Zheng@latrobe.edu.au, l.chi@latrobe.edu.au, K.Phan@latrobe.edu.au, phoebe.chen@latrobe.edu.au
- M. Jin and Y. Liu are with the Department of Data Science and AI, Faculty of IT, Monash University, Clayton, VIC 3800, Australia
E-mail: ming.jin@monash.edu; yixin.liu@monash.edu;
- Corresponding Authors: Ming Jin and Lianhua Chi.

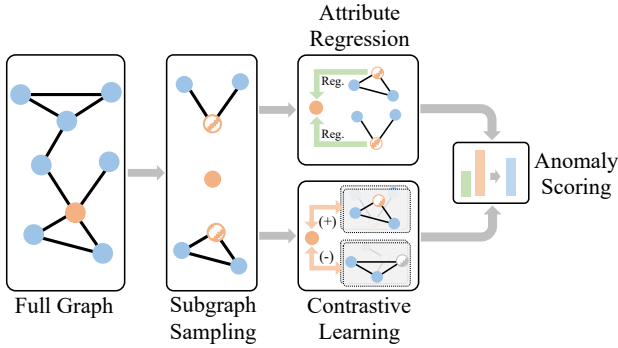


Fig. 1. The workflow chart of $SL-GAD$ on self-supervised graph anomaly detection. The abnormality of a node is estimated on twofold perspectives, namely generative and contrastive graph anomaly scoring.

anomaly detection. These autoencoder approaches typically aim to reconstruct the whole graph structure or attributes for every single node. As anomaly detection aims to “identify patterns in data that do not conform to *expected behaviour*” [9], it is natural to define the expected behaviour based the contextual information, which is largely ignored in existing methods. Furthermore, these algorithms do not fully exploit the available information as supervision signals to learn their models. The learning objective in these methods is mostly focused on the node level (e.g., learning node-level embedding directly from graph autoencoder). The subgraph information of a target node can provide more supervision signals and that are also not well exploited for graph anomaly detection.

Based on these observations, in this paper, we present a novel self-supervised algorithm, $SL-GAD$, for graph anomaly detection. Our theme is to construct different surrounding contexts (subgraphs) of a target node and employ self-supervised learning strategies to make comparison and obtain the anomaly score for each node. Specifically, we first sample different views (local subgraphs) centralised on each target node as the contextual information. These views are then fed into a graph neural network (GNN) encoder to learn the latent representation of each node. After this, we employ two modules, namely *generative attribute reconstruction* and *multi-view contrastive learning*, to fully exploit the available information in a self-supervised manner. By reconstructing node attributes with a GNN decoder, the *generative attribute reconstruction* module is able to capture anomalies in the attribute space. By directly comparing a target node with its surrounding contexts, the *multi-view contrastive learning* module can capture anomalies in the structure space and mix of both structure and content information. Finally, the anomaly score is calculated based on both generative and contrastive modules to provide a comprehensive score to qualify the abnormality of each node. Experimental results on six datasets show the effectiveness of our algorithm. A workflow chart of our model is given in Figure 1.

The main contribution of this paper can be summarised as follows.

- We propose a novel self-supervised based method for graph data. By developing a subgraph-based con-

trastive learning module, our method can effectively exploit the useful information in graphs.

- We develop a new method for graph anomaly detection. By developing both generative attribute regression and multi-view contrastive learning mechanisms, our method provides a new way to qualify the anomaly score for each node for anomaly detection.
- We have conducted extensive experimental results on six datasets to test our design for graph anomaly detection. Experimental results show that our algorithm outperforms state-of-the-art algorithms by a large margin.

The rest of the paper is organised as follows: Section 2 reviews the related work. Section 3 depicts the definition of the problem. Section 4 presents the proposed method. Section 5 discusses the experimental results and we conclude this paper in Section 6.

2 RELATED WORK

This work is closely related to graph anomaly detection, self-supervised learning, and graph representation learning. We briefly review these related works in this section.

2.1 Anomaly detection

Anomaly detection has been a long-standing research topic [9], [10]. Aiming to identify patterns that significantly differ from the expected patterns, research in this area has been evolving from traditional statistic methods such as local outlier factor [11] and one-class support vector machine [12] to deep learning approaches such as Outlier Exposure (OE) [13] and Deep Semi-Supervised Anomaly Detection (Deep SAD) [14]. While these methods typically target data in the Euclidean domain, recently, anomaly detection from graph structure data which are outside Euclidean space draws increasing attention [3], [4], [5], [15]. Because how to measure the anomaly is an important problem for anomaly detection in graphs, Perozzi and Akoglu [3] defined the normality as a measure and proposed an AMEN approach for anomaly detection. Exploiting the residual for anomaly detection, Li *et al.* proposed the Radar approach [4] and Peng *et al.* proposed the Anomalous approach [5] which employ matrix regression approach and regard nodes with large residual as anomalies. Recently, deep approaches have been also applied in graphs for anomaly detection [6], [7], [8]. These methods typically employ a graph autoencoder to embed the nodes in a latent space, and then reconstruct the graph information. The reconstruction errors are used to detect anomalies. Recently, Liu *et al.* proposed a self-supervised approach called CoLA [15], which exploits the local information from network data by sampling pairs of instance, and employs the contrastive learning to learn the node representation. The abnormal score is calculated based on the predicted scores on the contrastive pairs. However, CoLA only utilizes self-supervised learning in a contrastive manner to capture the anomaly patterns, which limits supervision signals to learn the model due to the lack of generative self-supervised learning.

2.2 Self-supervised learning

Self-supervised learning (SSL) [16] is a new learning paradigm which aims to learn a neural model from the unsupervised data itself without using human-annotated labels. By training on well-designed *pretext tasks*, SSL enables a model to learn better representations that can be generalized to downstream tasks. SSL has achieved great success on computer vision (CV) [17] and natural language processing (NLP) [16]. Recently, SSL has been extended to graph domains (please refer to [18] for a comprehensive survey for graph SSL). In particular, Veličković *et al.* proposed the first contrastive learning algorithm, Deep Graph Infomax (DGI) [19], to learn the embedding from graph data in an unsupervised manner. Hassani and Khasahmadi proposed an approach MVGRL [20] which performs contrastive learning on graphs from first-order neighbours and a graph diffusion on two views. Wan *et al.* proposed an algorithm CG³ [21] which exploits contrastive learning based on both graph structure and limited labelled information among nodes. By capitalizing on the idea of self-knowledge distillation, Jin *et al.* proposed a method MERIT [22] to enrich supervision signals by maximizing the agreement of node embeddings across different views and networks. JOAO [23], on the other hand, proposed to automatically learn graph augmentations with the self-supervised model, which alleviates the reliance on the design of augmentations. However, while all these algorithms only focus on learning the representation for nodes in graphs, they have not been applied for anomaly detection.

2.3 Graph representation learning

Our work is also related to *graph representation learning*, where the goal is to learn a representation for each node or the entire graph, so that downstream graph analysis tasks (such as node classification and anomaly detection) can be easily performed. Graph neural networks (GNNs) [24], particularly graph convolutional networks [25], [26], have achieved great success for this task. Kipf and Welling proposed the graph convolutional networks (GCNs) [25] which employs a two-level architecture and performs message passing in the spectral domain, showing impressive performance in the node classification task. Veličković *et al.* proposed a graph attention network (GAT) [26] which employs a neural network to automatically learn the weights (attentional scores) of each neighbour in the process of message passing, further improving the performance of GCN. To improve the scalability of graph neural networks, Hamilton *et al.* proposed a GraphSage algorithm [27] which performs sampling for the neighbour message aggregation. Differently, Frasca *et al.* proposed a method SIGN based on graph convolutional filters with different size [28], which alleviates the reliance on graph sampling. To improve the robustness of graph representation learning, Pan *et al.* proposed an adversarial regularised graph autoencoder (ARGA) which employs an adversarial training method to regularise the embedding in the latent space. Geisler *et al.*, on the other hand, proposed a robust aggregation function to learn robust graph representations [29]. To improve the rigidity and inflexibility of deterministic classification functions employed in existing GNN methods, Wang *et*

TABLE 1
Summary of the primary notations.

Symbols	Description
$\mathcal{G} = (\mathbf{X}, \mathbf{A})$	An attributed graph
\mathcal{V}, \mathcal{E}	The node and edge set of \mathcal{G}
$\mathbf{A} \in \mathbb{R}^{N \times N}$	The adjacency matrix of \mathcal{G}
$\mathbf{X} \in \mathbb{R}^{N \times D}$	The node features matrix of \mathcal{G}
$\mathbf{x}_i \in \mathbb{R}^D$	The feature vector of v_i that $\mathbf{x}_i \in \mathbf{X}$
$\mathcal{N}(v_i)$	The neighbors of node $v_i \in \mathcal{V}$
$v_t \in \mathcal{V}$	A selected target node
$\mathcal{G}_t^{\phi_1}, \mathcal{G}_t^{\phi_2}$	Two generated graph views of v_t
$\mathbf{X}_t^{\phi_i} \in \mathbb{R}^{K \times D}$	The node feature matrix of $\mathcal{G}_t^{\phi_i}$
$\widehat{\mathbf{X}}_t^{\phi_i}[-1, :] \in \mathbb{R}^D$	The reconstructed feature vector of anonymized target node in $\mathcal{G}_t^{\phi_i}$
$\mathbf{A}_t^{\phi_i} \in \mathbb{R}^{K \times K}$	The adjacency matrix of $\mathcal{G}_t^{\phi_i}$
$f(v_t)$	The anomaly score of v_t
$\mathbf{h}_t \in \mathbb{R}^{D'}$	The embedding vector of target node v_t
$\mathbf{g}_{\phi_i} \in \mathbb{R}^{D'}$	The graph embedding vector of $\mathcal{G}_t^{\phi_i}$
$\mathbf{H}_{\phi_i} \in \mathbb{R}^{K \times D'}$	The node embedding matrix of $\mathcal{G}_t^{\phi_i}$
$\mathbf{H}_{\phi_i}[j, :] \in \mathbb{R}^{D'}$	The embedding vector of v_j in \mathbf{H}_{ϕ_i}
$\mathbf{H}_{\phi_i}^{(l)} \in \mathbb{R}^{K \times D'_l}$	The node embedding matrix of $\mathcal{G}_t^{\phi_i}$ on the l -th GNN layer
$\mathbf{H}_{\phi_i}^{(l)}[j, :] \in \mathbb{R}^{D'_l}$	The embedding vector of v_j in $\mathbf{H}_{\phi_i}^{(l)}$
$\mathbf{W}_{enc} \in \mathbb{R}^{D \times D}$	The trainable parameter matrix of graph encoder
$\mathbf{W}_{dec} \in \mathbb{R}^{D \times D}$	The trainable parameter matrix of graph decoder
$\mathbf{W}_s \in \mathbb{R}^{D' \times D'}$	The trainable parameter matrix of contrastive discriminator
N	The number of nodes in \mathcal{G}
K	The number of nodes in graph views
D	The dimension of node features in \mathcal{G}
D'	The dimension of embeddings in \mathbf{H}_{ϕ_i}
D'_l	The dimension of embeddings in $\mathbf{H}_{\phi_i}^{(l)}$
R	The number of evaluation rounds to calculate final anomaly scores

al. proposed a novel framework named Graph Stochastic Neural Networks (GSNN) [30], which aims to model the uncertainty of the classification function by simultaneously learning a family of functions, i.e., a stochastic function. As many GNNs lack the flexibility to model intrinsic complex graph geometry by embedding graphs into either Euclidean or hyperbolic spaces, a graph geometry interaction learning algorithm (GIL) [31] is proposed recently to utilize the strength of both Euclidean and hyperbolic geometries. Wu *et al.* proposed an algorithm [32] to handle data in a positive and unlabelled learning setting, in which only part of the nodes are labelled as positive nodes and the majority of nodes are unlabelled nodes. Graph representation learning techniques have also been widely applied in heterogeneous networks [33], spatial-temporal networks [34], community detection [35], and image classification [36]. However, existing GNNs approaches are mostly focused on generic graph representation learning. Employing GNNs for anomaly detection is still under-explored. By integrating GNNs with self-supervised learning, we will develop a new approach for graph anomaly detection in this paper.

3 PROBLEM DEFINITION

In this section, we introduce the unsupervised graph anomaly detection problem and notations used in the paper. Specifically, we use bold uppercase and lowercase letters to denote matrices and vectors, respectively. All important notations have been summarized in Table 1. Graph and graph neural network (GNN) are defined as follows:

Definition 3.1 (Graph). Given an attributed graph $\mathcal{G} = (\mathbf{X}, \mathbf{A})$, we use $\mathbf{X} \in \mathbb{R}^{N \times D}$ and $\mathbf{A} \in \mathbb{R}^{N \times N}$ to denote the node features and graph adjacency matrix, where $N = |\mathcal{V}|$ and $\mathcal{V} = \{v_1, v_2, \dots, v_N\}$ is a set of nodes in the graph. Specifically, we use $\mathbf{x}_i \in \mathbb{R}^D$ to symbolize the feature of node v_i . Let \mathcal{E} denotes a set of graph edges, where $e_{ij} = \{v_i, v_j\} \in \mathcal{E}$ is an edge between node v_i and v_j . The underlying graph structure is represented by a $N \times N$ square matrix \mathbf{A} , where $\mathbf{A}_{ij} = 1$ if $e_{ij} = \{v_i, v_j\}$, otherwise $\mathbf{A}_{ij} = 0$. Particularly, the neighborhood of a node v is defined as $\mathcal{N}(v) = \{u \in \mathcal{V} | e_{vu} \in \mathcal{E}\}$.

Definition 3.2 (Graph Neural Networks). Given an attributed graph $\mathcal{G} = (\mathbf{X}, \mathbf{A})$, a graph neural network $GNN(\cdot)$ aims to learn a local aggregation rule to map the original node features $\mathbf{X} = \{\mathbf{x}_1, \mathbf{x}_2, \dots, \mathbf{x}_N\} \in \mathbb{R}^{N \times D}$ to low-dimensional representations (i.e., embeddings) $\mathbf{H} = \{\mathbf{h}_1, \mathbf{h}_2, \dots, \mathbf{h}_N\} \in \mathbb{R}^{N \times D'}$.

In this paper, we mainly focus on the problem of unsupervised anomaly detection on attributed graphs, which is defined below:

Definition 3.3 (Unsupervised Graph Anomaly Detection). Provided an attributed graph $\mathcal{G} = (\mathbf{X}, \mathbf{A})$, we aim to learn a model $\mathcal{F}(\cdot) : \mathbb{R}^{N \times D} \rightarrow \mathbb{R}^{N \times 1}$, which measures the degree of abnormality of a node in the graph by calculating its anomaly score without relying on any labelling information. Thus, the main task is to rank nodes according to their anomaly scores in a descending order, where anomalies can be easily detected based on this ranking list.

4 METHODOLOGY

In this section, we present the overall framework of our proposed algorithm SL-GAD to detect node-level graph anomalies in an unsupervised manner. As shown in Figure 2, our method has three different components, including *graph view sampling*, *generative and contrastive self-supervised learning*, and *graph anomaly scoring*. Firstly, we select a target node from the input graph, then we exploit the contextual information for this node. Specifically, we generate two associated graph views by leveraging different augmentations. After this, to fully utilize the rich node- and subgraph-level information to detect anomalies, we construct two different self-supervised objectives, namely *generative attribute reconstruction* and *multi-view contrastive learning*. The former objective is inspired by the idea of graph auto-encoder (GAE) [37], which aims to reconstruct the feature vector of target node based on its neighboring attributive information. In such a way, if a selected target node is an anomaly, the attributive mismatch between it and its surrounding contexts can be reflected as the regression loss between its reconstructed and original feature vector. Similar to but

different from this node-level generative objective, we introduce another mixed-level contrastive objective to compare a target node with its surrounding contexts directly on the embedding and structure space, which injects richer structural information during the discrimination. As a result, our model optimizes two self-supervised objectives that are closely related to the graph anomaly detection. During the inference, two scoring functions are elaborately designed based on the aforementioned two objectives, which tend to assign attributive and structural anomalies in a graph with higher anomaly scores.

In the rest of this section, we introduce the three core components of SL-GAD from Subsection 4.1 to 4.4. In Subsection 4.5, we present and analyse the training objective, algorithm, and its time complexity.

4.1 Graph View Establishment for Anomaly Detection

Recent work in graph self-supervised learning suggests that the design of discrimination pairs is the key to allow graph encoders extracting rich structural and attributive information [20], [38], [39], [40]. Similar to the visual domain, graph self-supervised learning can be roughly divided into two categories: Generative-based and Contrastive-based. As for the generative branch, existing work mainly lies on the attributive and structural auxiliary property prediction [18], where the comparisons are typically placed on the same scale, such as "node v.s. node" (e.g., attribute regression) and "graph v.s. graph" (e.g., structure prediction). On the other hand, contrastive learning could discriminate instances not only from the same but also across different scales, such as "node v.s. graph" in [20] and [41]. However, not all of aforementioned discriminations are applicable to our task because graph anomaly detection and representation learning are two fundamentally different tasks. In graph anomaly detection, inspired by [15], we conjecture that an anomaly is typically reflected as the mismatch between it and its surrounding contexts, which forms the foundation of our graph view construction.

In our method, to establish the connection between a target node and its surrounding contexts, we propose two self-supervised learning objectives from different scales and spaces. Specifically, we first conduct the node-level discrimination, which reconstructs the feature vector of a target node by leveraging a GAE and then compares it with ground truth in the attribute space. To inject richer structural information, we further construct a mixed-level contrastiveness between a target node and its local subgraphs in the embedding and structure space, where sampling multiple views benefits our contrastive module exploring diverse semi-global (i.e., surrounding contextual) information during its discrimination [42]. Based on this, as shown in the leftmost part in Figure 2, we first sample a target node from the input graph, and then we sample two different views (local subgraphs) around it by leveraging different graph augmentations. Although it is possible to equip SL-GAD with more than two views, it may introduce redundant information depending on the choice of augmentations [20], [43] and thus degrading model performance.

For our generative objective, the discrimination pair is the original and reconstructed target node. On the other

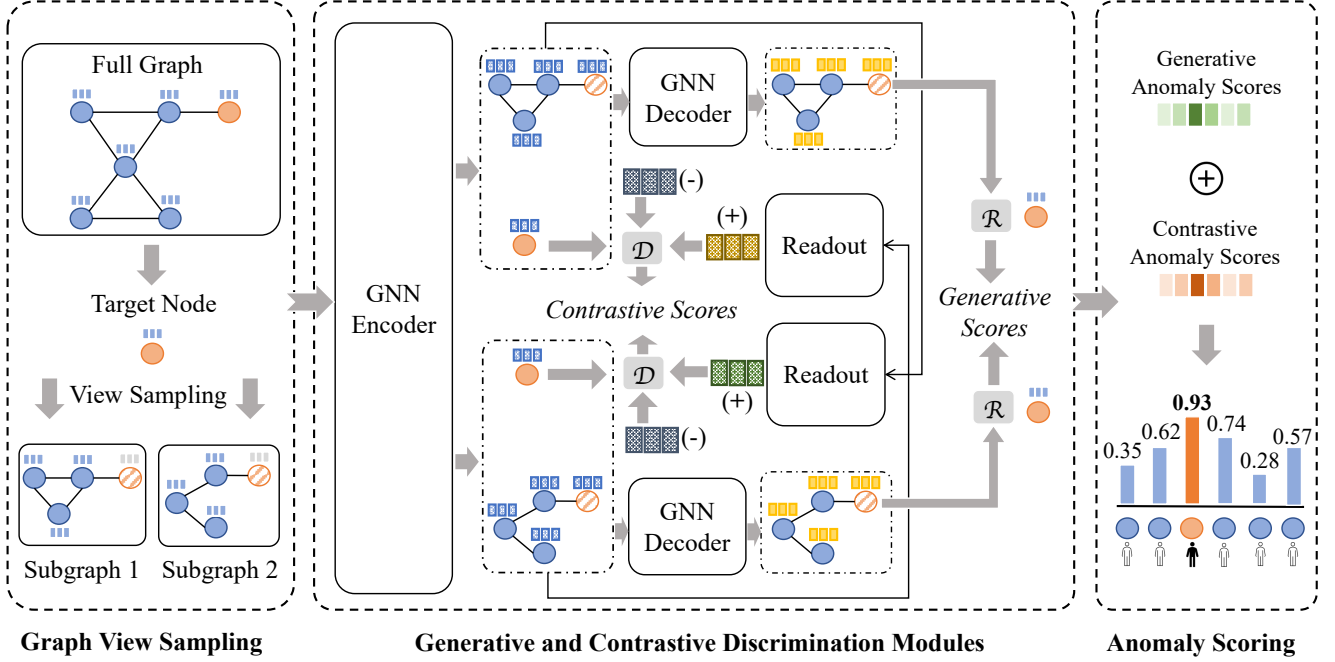


Fig. 2. The conceptual framework of $SL\text{-}GAD$, which consists of three main components: Graph view sampling, self-supervised discrimination, and graph anomaly scoring. Orange and blue nodes denote the abnormal and normal nodes in a given graph. Firstly, a selected target node and two sampled subgraphs are encoded via a GNN encoder in the leftmost part. After this, two self-supervised objectives are introduced in the middle part, where \mathcal{D} and \mathcal{R} are shared discriminators and regressors. The GNN decoder are also shared across two graph views. Finally, in the rightmost part, we calculate the anomaly score for each node from two sources, where the anomalies can be easily detected (e.g., the orange node).

hand, the target node and two sampled graph views consist of two discrimination pairs in our contrastive objective. Now we give a detailed explanation of the aforementioned processing steps:

- 1) **Target node sampling.** Since we mainly focus on detecting node-level anomalies in graphs, a target node needs to be sampled first. In this paper, we sample a target node from the given input graph via the uniform sampling without replacement.
- 2) **Graph view sampling.** Although several augmentations have been proposed on graphs, such as node feature masking and edge modification [22], these augmentations are not applicable to graph anomaly detection because they introduce extra anomalies (e.g., modifying the underlying linkages and node features). Alternatively, in this paper, we leverage random walks with restart (RWR) [44] as augmentations, which avoid violating the underlying graph semantic information. Specifically, this approach samples graph views centered at a target node with the fixed size K , which controls the radius of surrounding contexts. It worths noting that graph diffusion [45] could also be a possible augmentation in our method to further injects the global information into our multi-view contrastiveness, which we leave in our future work.
- 3) **Graph view anonymization.** The target node in sampled graph views is anonymized (i.e., its features have been zeroed) to increase the difficulty of two predefined self-supervised learning pretext tasks, which helps facilitate the model training [18], [46]. In such a way, the raw attributive information of the target node will not contribute to its feature reconstruction, as well as the

calculation of graph view embeddings. This mechanism prevents the information leakage and encourages the model to identify anomalies by relying on the contextual information.

4.2 Generative Learning with Attribute Reconstruction

As suggested in [6], the abnormality of an instance can be typically reflected as the degree of mismatch between its original and reconstructed information. Specifically, this type of mismatch can be quantified by the l_2 -norm distance, where a higher distance denotes a higher reconstruction error, indicating that the given instance is more likely to be an anomaly. Among existing anomaly detection methods, deep autoencoder (AE) [47] has shown a strong performance. AE is a type of neural network that has been firstly introduced to learn latent representations in an unsupervised manner, which consists of two components: Deep encoder and decoder. Given an input feature vector \mathbf{x} , a typical AE can be defined as:

$$\mathbf{x}' = AE(\mathbf{x}) = f_{dec}(f_{enc}(\mathbf{x})), \quad (1)$$

where $\mathbf{x}' = f_{dec}(\mathbf{h})$ and $\mathbf{h} = f_{enc}(\mathbf{x})$ are deep decoder and encoder, respectively. In above equation, \mathbf{x}' is the reconstructed feature vector, and \mathbf{h} denotes the latent representation of \mathbf{x} . The optimization objective of AE is to make \mathbf{x}' and \mathbf{x} as close as possible, which can be achieved by minimizing their l_2 -norm distance, i.e., $\|\mathbf{x}' - \mathbf{x}\|_2^2$, to encourage AE to learn latent invariant patterns among inputs.

However, in the context of graph anomaly detection, a conventional AE only reconstructs the attributive information of a node and fails to take the underlying

topological information into the consideration, which makes it unfavorable to this task. To alleviate this limitation, as shown in the middle part of Figure 2, we construct a GAE with two components: GNN-based encoder and decoder.

GNN-based encoder. Given two graph views $\mathcal{G}_t^{\phi_1}$ and $\mathcal{G}_t^{\phi_2}$ of a target node v_t , we resort to transform their high-dimensional node features to low-dimensional representations via a GNN encoder, which is formulated as:

$$\mathbf{H}_{\phi_i} = \text{GNN}_{enc}(\mathbf{X}_t^{\phi_i}, \mathbf{A}_t^{\phi_i}), \quad (2)$$

where \mathbf{H}_{ϕ_i} , $\mathbf{X}_t^{\phi_i}$, and $\mathbf{A}_t^{\phi_i}$ denote the node embedding matrix, node feature matrix, and adjacency matrix of $\mathcal{G}_t^{\phi_i}$, respectively. $\text{GNN}_{enc}(\cdot)$ is the graph encoder, which consists of a L -layer GNN. Specifically, we define it as follows:

$$\begin{aligned} \mathbf{m}_{\phi_i}^{(l)}[j, :] &= \text{AGGREGATE}^{(l)}(\mathbf{H}_{\phi_i}^{(l-1)}[k, :] : v_k \in \mathcal{N}(v_j)), \\ \mathbf{H}_{\phi_i}^{(l)}[j, :] &= \text{COMBINE}^{(l)}(\mathbf{H}_{\phi_i}^{(l-1)}[j, :], \mathbf{m}_{\phi_i}^{(l)}[j, :]), \end{aligned} \quad (3)$$

where $\mathbf{H}_{\phi_i}^{(l)}[j, :]$ denotes the latent vector of v_j in $\mathbf{H}_{\phi_i}^{(l)}$, which is the latent representation of $\mathcal{G}_t^{\phi_i}$ at the l -th layer. In particular, $\mathbf{H}_{\phi_i} = \mathbf{H}_{\phi_i}^{(L)}$ and $\mathbf{X}_t^{\phi_i} = \mathbf{H}_{\phi_i}^{(0)}$. In the above formulas, we use $\mathbf{m}_{\phi_i}^{(l)}[j, :]$ to denote the aggregated message of v_j in $\mathcal{G}_t^{\phi_i}$ at the l -th layer. $\text{AGGREGATE}^{(l)}(\cdot)$ and $\text{COMBINE}^{(l)}(\cdot)$ are message aggregation and combination (a.k.a. transformation) functions in a typical GNN layer.

In this paper, for simplicity, we apply a one-layer GCN [25] as our backbone graph encoder. In such a way, Equation (2) can be specifically formulated as:

$$\mathbf{H}_{\phi_i} = \text{GNN}_{enc}(\mathbf{X}_t^{\phi_i}, \mathbf{A}_t^{\phi_i}) = \sigma(\widehat{\mathbf{A}}_t^{\phi_i} \mathbf{X}_t^{\phi_i} \mathbf{W}_{enc}), \quad (4)$$

where $\widehat{\mathbf{A}}_t^{\phi_i} = (\widetilde{\mathbf{D}}_t^{\phi_i})^{-\frac{1}{2}} \widetilde{\mathbf{A}}_t^{\phi_i} (\widetilde{\mathbf{D}}_t^{\phi_i})^{-\frac{1}{2}}$, $\widetilde{\mathbf{A}}_t^{\phi_i} = \mathbf{A}_t^{\phi_i} + \mathbf{I}$, and $\widetilde{\mathbf{D}}_t^{\phi_i}[i, i] = \sum_j \mathbf{A}_t^{\phi_i}[i, j]$. Specifically, $\sigma(\cdot)$ denotes a non-linear activation function (e.g., ReLU), and \mathbf{W}_{enc} is a trainable parameter matrix in our graph encoder.

GNN-based decoder. Similarly, we build our graph decoder with a single GCN layer, which is slightly different from Equation (4). During the attribute reconstruction, we take node embedding matrix as the input and then reconstruct the node features accordingly:

$$\widehat{\mathbf{X}}_t^{\phi_i} = \text{GNN}_{dec}(\mathbf{H}_{\phi_i}, \mathbf{A}_t^{\phi_i}) = \sigma(\widehat{\mathbf{A}}_t^{\phi_i} \mathbf{H}_{\phi_i} \mathbf{W}_{dec}), \quad (5)$$

where \mathbf{W}_{dec} is a trainable parameter matrix in our graph decoder.

Generative graph anomaly detection. By aggregating the neighboring information, the attributive reconstruction of $\mathcal{G}_t^{\phi_1}$ and $\mathcal{G}_t^{\phi_2}$ is mainly based on the attributive information of local surrounding subgraphs centred at v_t . In this paper, we anonymize the target node v_t in its two graph views to enforce its attributive reconstruction purely based on the contextual information. As we mentioned, this schema better reflects node-level anomalies in the attribute space. Thus, we propose to minimize the Mean Squared Error (MSE) between target node's original and reconstructed features in two graph views, as shown in Figure 2.

$$\mathcal{L}_{gen}^j = \frac{1}{N} \sum_{i=1}^N (\widehat{\mathbf{X}}_i^{\phi_j}[-1, :], \mathbf{x}_i)^2, \quad j \in \{1, 2\}, \quad (6)$$

where \mathbf{x}_i is the feature vector of a target node v_i , and $\widehat{\mathbf{X}}_i^{\phi_j}[-1, :]$ denotes the reconstructed feature vector of anonymized target node v_i in its j -th graph view. Specifically, $\widehat{\mathbf{X}}_i^{\phi_j}$ can be obtained via Equation (4) and (5). Finally, we have our generative objective by combining \mathcal{L}_{gen}^j in Equation (6):

$$\mathcal{L}_{gen} = \frac{1}{2} (\mathcal{L}_{gen}^1 + \mathcal{L}_{gen}^2). \quad (7)$$

4.3 Multi-View Contrastive Learning

As we mentioned before, node anomalies are typically reflected as the mismatch between nodes and their surrounding contexts. Our generative module identifies anomalies in the attribute space with the help of our GNN encoder and decoder, but the structural information has not been directly utilized. To overcome this limitation and inject richer structural information, we propose a multi-view contrastive module, which contrasts a target node with two associated graph views directly. Different from the generative objective where the discrimination is placed on the node-level and in the attribute space, our multi-view contrastive learning mixes different graph topological scales, which discriminates the representation of a target node with its local subgraph representations in the embedding and structural space, emphasizing more on semi-global information. As illustrated in Figure 2, our contrastive module mainly consists of three different components: Graph encoder, readout module, and contrastive module.

GNN-based encoder. Our contrastive module takes the node feature vector and matrices of a selected target node and two associated graph views as the input, where the underlying graph encoder shares the same parameters with the generative module. The encoding of two graph views has been formulated in Equation (4), while the transformation of target node feature vector follows a different formula:

$$\mathbf{h}_t = \sigma(\mathbf{x}_t \mathbf{W}_{enc}), \quad (8)$$

where \mathbf{h}_t and \mathbf{x}_t are embedding and feature vectors of the target node v_t . It is worth noting that a single target node has no underlying graph structure, so the graph adjacency matrix in Equation (4) is discarded in Equation (8). Thus, Equation (8) is equivalent to a non-linear mapping of \mathbf{x}_t , where \mathbf{W}_{enc} is shared with Equation (4).

Readout module. Since we aim to contrast \mathbf{h}_t with the surrounding subgraphs directly, we are motivated to design a readout module to generate two semi-global (subgraph-level) representations based on \mathbf{H}_{ϕ_1} and \mathbf{H}_{ϕ_2} , as shown in the middle part of Figure 2.

In general, several readout functions are commonly used to generate graph-level representations based on node-level embeddings, such as average and differentiable pooling [20], [48]. For simplicity, we adopt the average pooling in this paper, which can be formulated as:

$$\mathbf{g}_{\phi_i} = \frac{1}{K} \sum_{j=1}^K \mathbf{H}_{\phi_i}[j, :], \quad (9)$$

where \mathbf{g}_{ϕ_i} denotes the graph-level embedding vector of view $\mathcal{G}_t^{\phi_i}$. K is the number of nodes in a graph view.

Contrastive module. Given \mathbf{h}_t , \mathbf{g}_{ϕ_1} , and \mathbf{g}_{ϕ_2} , we aim to discriminate them pairwise. Specifically, we first formulate the positive and negative pairs of v_t as follows:

$$P_t^{\phi_i} = (\mathbf{h}_t, \mathbf{g}_{\phi_i}), \quad (10)$$

$$\tilde{P}_t^{\phi_i} = (\mathbf{h}_t, \tilde{\mathbf{g}}_{\phi_i}), \quad (11)$$

where $P_t^{\phi_i}$ and $\tilde{P}_t^{\phi_i}$ are positive and negative pairs of the selected target node v_t . In Equation (11), $\tilde{\mathbf{g}}_{\phi_i}$ denotes the negative samples, which are the representations of randomly cropped subgraphs from \mathcal{G} and different from $\mathcal{G}_t^{\phi_1}$ and $\mathcal{G}_t^{\phi_2}$.

To contrast two elements in positive and negative pairs, we design a discriminator based on the bilinear transformation [15], where the discrimination scores of $P_t^{\phi_i}$ and $\tilde{P}_t^{\phi_i}$ are defined as follows:

$$s_t^{\phi_i} = \sigma(\mathbf{h}_t \mathbf{W}_s \mathbf{g}_{\phi_i}^\top), \quad (12)$$

$$\tilde{s}_t^{\phi_i} = \sigma(\mathbf{h}_t \mathbf{W}_s \tilde{\mathbf{g}}_{\phi_i}^\top), \quad (13)$$

where $s_t^{\phi_i}$ and $\tilde{s}_t^{\phi_i}$ are contrastive discrimination scores of the pairs $P_t^{\phi_i}$ and $\tilde{P}_t^{\phi_i}$. In the above equations, $\mathbf{W}_s \in \mathbb{R}^{D' \times D'}$ is a learnable scoring matrix, which measures the similarity between two input vectors. Particularly, we resort to use the sigmoid function as our non-linear transformation $\sigma(\cdot)$ in above two equations to ensure our discrimination scores fall within the range $[0, 1]$.

Multi-view contrastive graph anomaly detection. Conceptually, graph anomalies should be different from their surrounding contexts on both attributive and topological perspectives. Thus, we conjecture that $s_t^{\phi_i}$ should be significantly larger than $\tilde{s}_t^{\phi_i}$, which indicates that for most of normal nodes in \mathcal{G} , target node representations (e.g., \mathbf{h}_t) should share more similarities with their surrounding contexts (e.g., \mathbf{g}_{ϕ_i}) than other subgraphs (e.g., $\tilde{\mathbf{g}}_{\phi_i}$).

Motivated by this, we form our multi-view contrastive objectives based on the Jensen-Shannon divergence [38], which maximizes the agreement between a target node and its surrounding contexts:

$$\mathcal{L}_{con}^j = -\frac{1}{2N} \sum_{i=1}^N (\log(s_i^{\phi_j}) + \log(1 - \tilde{s}_i^{\phi_j})), \quad j \in \{1, 2\}, \quad (14)$$

where \mathcal{L}_{con}^j denotes the contrastive loss of graph view j across all nodes in \mathcal{G} . By combining \mathcal{L}_{con}^j in Equation (14), we have our final contrastive objective:

$$\mathcal{L}_{con} = \frac{1}{2} (\mathcal{L}_{con}^1 + \mathcal{L}_{con}^2). \quad (15)$$

4.4 Graph Anomaly Scoring

Until now, we have introduced two different self-supervised discrimination schemes for graph anomaly detection by leveraging our generative and contrastive modules to compare nodes with their contextual information. As the majority of nodes in \mathcal{G} are not anomalies, a well-trained graph encoder and decoder are expected to map the feature vector

of a normal node to an appropriate latent space and vice versa. For anomalies in \mathcal{G} , their embeddings and reconstructed features are likely to be distorted because of their attributive or structural abnormalities.

For the generative learning, the attributive reconstruction of an anonymized target node is purely based on its local (i.e., neighbouring) contextual information, where the degree of mismatch between the reconstructed and original feature vector is an ideal metric to measure the abnormality of a node. In this paper, we adopt the ℓ_2 -norm distance as the generative anomaly scoring function. For a node $v_i \in \mathcal{V}$, we define this function as follows:

$$f_{gen}(v_i) = \frac{1}{2} \sum_{j=1}^2 \left(\delta^1 (\|\hat{\mathbf{X}}_i^{\phi_j}[-1, :] - \mathbf{x}_i\|_2^2) \right), \quad (16)$$

where $f_{gen}(v_i)$ denotes the generative anomaly score of v_i . In above formula, $\hat{\mathbf{X}}_i^{\phi_j}[-1, :]$ is the reconstructed feature vector of v_i , which is calculated in Equation (5). Specifically, δ^1 denotes a scaler, which scales a ℓ_2 -norm distance to the range of $[0, 1]$. In such a way, if v_i is an anomaly, $f_{gen}(v_i)$ is expected to be close to 1, otherwise this score should be close to 0.

However, our generative learning focuses only the node-level discrimination on the attribute space, where the graph topological information has not been directly utilized. To overcome this limitation, our contrastive module discriminates a target node with the surrounding subgraphs directly on the embedding space, where the discrimination scores in Equation (12) and (13) can be naturally combined to form an abnormality metric. Inspired by [15], for a node $v_i \in \mathcal{V}$, we define our contrastive anomaly scoring function as follows:

$$f_{con}(v_i) = \frac{1}{2} \sum_{j=1}^2 \delta^2 \left(\tilde{s}_i^{\phi_j} - s_i^{\phi_j} \right), \quad (17)$$

where $f_{con}(v_i)$ denotes the contrastive anomaly score of v_i . Specifically, $s_i^{\phi_j}$ and $\tilde{s}_i^{\phi_j}$ are positive and negative contrastive discrimination scores defined in Equation (12) and (13). If v_i is a normal node, $s_i^{\phi_j}$ is expected to be close to 1, and $\tilde{s}_i^{\phi_j}$ is likely to be close to 0. Otherwise, if v_i is an anomaly, $s_i^{\phi_j}$ and $\tilde{s}_i^{\phi_j}$ are expected to be close to 0.5 because of the mismatch between v_i and its surrounding subgraphs. Thus, $\tilde{s}_i^{\phi_j} - s_i^{\phi_j}$ falls in the range of $[-1, 0]$. By introduce a scaler δ^2 , our final contrastive anomaly scores will be scaled to the range of $[0, 1]$.

By combining aforementioned two anomaly scoring functions, we have our final graph anomaly scoring function to estimate the abnormality of a node $v_i \in \mathcal{V}$:

$$f(v_i) = \alpha f_{con}(v_i) + \beta f_{gen}(v_i), \quad (18)$$

where α and β are two tunable balancing factors to weight the importance of contrastive and generative scoring functions. In practice, as suggested in [15], we may have to repeat this calculation R times to obtain a statistical stable anomaly score. This is because two sampled graph views $\mathcal{G}_t^{\phi_1}$ and $\mathcal{G}_t^{\phi_2}$ are partial observations on v_t 's contextual information, which may be insufficient to estimate the abnormality of v_t .

Algorithm 1 The Proposed SL-GAD Algorithm

Input: Attributed graph \mathcal{G} ; Maximum training epochs E ; Batch size B ; Number of evaluation rounds R .
Output: Graph anomaly scoring function $f(\cdot)$.

- 1: Randomly initialize the trainable parameters \mathbf{W}_{encr} , \mathbf{W}_{decr} and \mathbf{W}_s ;
- 2: // Training stage
- 3: **for** $e \in 1, 2, \dots, E$ **do**
- 4: $\mathcal{B} \leftarrow$ Randomly split \mathcal{V} into batches with size B ;
- 5: **for** batch $b = (v_1, \dots, v_B) \in \mathcal{B}$ **do**
- 6: Sample two graph views for each of node in b , i.e., $(\mathcal{G}_1^{\phi_1}, \dots, \mathcal{G}_B^{\phi_1})$ and $(\mathcal{G}_1^{\phi_2}, \dots, \mathcal{G}_B^{\phi_2})$;
- 7: Calculate node and associated graph view embeddings via Eq. (8) and (4);
- 8: Calculate the reconstructed feature vectors for nodes in b via Eq. (5);
- 9: Calculate the loss \mathcal{L} via Eq. (7), (15), and (19);
- 10: Back propagation and update trainable parameters \mathbf{W}_{encr} , \mathbf{W}_{decr} and \mathbf{W}_s ;
- 11: **end for**
- 12: **end for**
- 13: // Inference stage
- 14: **for** $v_i \in \mathcal{V}$ **do**
- 15: **for** evaluation round $r \in 1, 2, \dots, R$ **do**
- 16: Calculate $f(v_i)$ via Eq. (16), (17), and (18);
- 17: **end for**
- 18: Average $f(v_i)$ over R evaluation rounds and output the final anomaly score for v_i ;
- 19: **end for**

4.5 Model Optimization and Algorithm

By combining our generative and contrastive objectives in Equation (7) and (15), we have our final optimization goal:

$$\mathcal{L} = \alpha \mathcal{L}_{con} + \beta \mathcal{L}_{gen}, \tag{19}$$

where \mathcal{L} is the training loss to be minimized. α and β are two balancing factors, which are the same as in Equation (18) to balance the importance of two self-supervised modules.

The overall procedures of the proposed SL-GAD are summarized in Algorithm 1. Firstly, we sample a batch of nodes from the input graph. For each of node, we generate two graph views. After this, nodes in a batch and associated graph views are encoded via a trainable GNN encoder. To calculate the generative loss, the node embeddings of graph views are decoded via a GNN decoder, where we aim to reconstruct the feature vector of anonymized target node in each graph view. Then, we compare the reconstructed feature vector of a node with its original feature vector. Simultaneously, the node embeddings of graph views are aggregated to generate view representations, which are then compared with the target node embeddings to calculate the contrastive loss. Finally, by combining two different objectives, we calculate the final training loss, where different trainable parameters can be updated via backpropagation. During the inference, the anomaly score of each node in \mathcal{G} will be repetitively calculated R times with different graph views sampled each time, which ensures the final anomaly scores are statistically stable.

4.5.1 Complexity Analysis

In this subsection, we analyse the time complexity of the proposed SL-GAD algorithm. For graph view sampling on a selected target node v_t , the time complexity of our RWR-based approach is $\mathcal{O}(\eta K)$, where η denotes the average node degree in the graph. Given a graph view $\mathcal{G}_t^{\phi_i}$ with K nodes, the time complexity of the proposed two self-supervised learning modules is $\mathcal{O}(K^2)$. Thus, considering a graph with N nodes, the training complexity of our algorithm is $\mathcal{O}(NK(\eta + K))$. During the inference, our graph anomaly scoring has a constant time complexity. Considering we have R evaluation rounds, the time complexity of our algorithm is $\mathcal{O}(RNK(\eta + K))$ when considering both model training and inference.

5 EXPERIMENTAL STUDY

In this section, we conduct comprehensive experiments on six real-world benchmark datasets to demonstrate the effectiveness of our proposed SL-GAD model. We compare our method with the state-of-the-art anomaly detection and self-supervised learning methods, and follow their configurations to carry out our experiments for a fair comparison. We conduct ablation study and parameter sensitivity experiments to further investigate the property of SL-GAD.

TABLE 2
The statistics of the datasets. The upper two datasets are social networks, and the remainders are citation networks.

Dataset	Nodes	Edges	Features	Anomalies
BlogCatalog [49]	5,196	171,743	8,189	300
Flickr [49]	7,575	239,738	12,407	450
ACM [50]	16,484	71,980	8,337	600
Cora [51]	2,708	5,429	1,433	150
CiteSeer [51]	3,327	4,732	3,703	150
Pubmed [51]	19,717	44,338	500	600

5.1 Dataset Description

To evaluate the performance of SL-GAD and the competitors, six real-world graph datasets, including two social network datasets and four citation network datasets, are utilized as benchmarks in our experiments. We provide the description of these datasets as follows:

- **Social Networks.** Blogcatalog and Flickr¹ [49] are two social network datasets whose data are collected from the blog sharing website BlogCatalog and the image sharing website Flickr, respectively. In these social network datasets, each node represents a user of websites, and each link indicates the following relationships between two users. The personalized contents (e.g., posting blogs or sharing photos with tag descriptions) of users are extracted as node features.
- **Citation Networks.** Cora, CiteSeer, Pubmed² [51] and ACM [50] are four public citation graph datasets. The data is collected from the corresponding publication databases. In these graphs, each node is a

1. <http://socialcomputing.asu.edu/pages/datasets>
 2. <http://linqs.cs.umd.edu/projects/projects/lbc>

published paper, while each edge denotes a citation relationship between two papers. The text contents of each paper are treated as its node features.

Since no ground-truth anomalies are included in these datasets, we need to inject synthetic anomalous data into the original data manually. To compare fairly, we follow the anomaly generation strategy used in [6] and [15]. Specifically, when injecting attributive anomalies, we select N_a nodes and then replace their features with randomly selected distant nodes' features. After this, we further inject equal number of structural anomalies into six datasets by selecting N'_a nodes and making them fully connected. We repeat this process q times such that $N_a = q \times N'_a$. The total numbers of anomalies are also summarized in Table 2 together with the dataset statistics.

5.2 Experimental Setup

We illustrate the experimental setup in this subsection, including baseline methods, evaluation metrics, and parameter settings.

Baselines. We compare SL-GAD against five state-of-the-art anomaly detection and self-supervised learning methods. We briefly introduce these methods as follows:

- **AMEN** [3] detects anomalies via ego-network analysis. It evaluates the correlation of attributes among different nodes within a ego-network to discriminate anomalous information.
- **Radar** [4] leverages residual analysis to identify the anomalies in graphs. It considers the residuals of attribute information and the coherence information with graph to detect anomalies.
- **ANOMALOUS** [5] learns the patterns of anomalies by considering the CUR decomposition and residual analysis. A joint learning framework is conducted to select informative attribute to detect anomalies.
- **DOMINANT** [6] is a deep learning-based graph anomaly detection method. It leverages a graph autoencoder to reconstruct the adjacency matrix and feature matrix simultaneously to learn the normal patterns of graph. Then, the abnormality of each node is measured by the reconstruction error of node.
- **DGI** [52] is a representative self-supervised learning method based on unsupervised contrasting. It learn node representation by maximizing the embedding agreement between each node and the full graph. For this method, we leverage its trained bilinear discriminator with Equation (17) to score node abnormalities.
- **CoLA** [15] is a contrastive self-supervised learning-based anomaly detection method. It captures anomaly patterns by evaluating the agreement between each node and its neighboring subgraph with a GNN-based encoder model.

Metrics. We utilize ROC-AUC, a widely applied metric for anomaly detection, to quantify the performance of SL-GAD and the competitors. The ROC curve indicates the plot of true positive rate (an anomaly is recognized as an anomaly) against false positive rate (a normal node is recognized as an anomaly). AUC is a value within a range

$[0, 1]$, which denotes the area under the ROC curve. A larger AUC value indicates a higher detection performance.

Parameter Settings. We set the sampled subgraph size K to be 4 for efficiency consideration. The GNN encoder is a one-layer GCN model, where hidden dimension D' is 64. α is fixed to 1 for all datasets, while β is selected from $\{0.2, 0.4, 0.6, 0.8, 1\}$. The discrimination modules are trained with Adam optimizer. Cora, Citeseer, Pubmed, and Flickr have learning rates of 0.001, BlogCatalog has 0.003, and ACM has 0.0005. The epoch number for BlogCatalog, Flickr and ACM are 400, and which for Cora, Citeseer and Pubmed are 100. The round number R for evaluation is 256.

5.3 Comparison with the State-of-the-art Methods

We compare our proposed SL-GAD with the six baseline methods in this subsection. The comparison of ROC curves is demonstrated in Figure 3, and the results of AUC values are illustrated in Table 3. According to these results, we summarize our observations as follows:

- The proposed method SL-GAD outperforms all the baseline methods on all benchmark datasets, demonstrating its capability to detect anomalies on graph data with high-dimensional node features. The reason behind this is that SL-GAD captures the anomaly patterns by jointly utilizing both generative and contrastive self-supervised learning.
- The shallow methods (AMEN, Radar, and ANOMALOUS) do not show a competitive anomaly detection performance in our experiments. This is because these mechanisms have limited capability to discriminate anomalies from graphs with high-dimensional features and complex structures, which results in relatively poor performance.
- Compared to other deep methods, SL-GAD shows a stronger detection performance and generalization ability. A possible reason is that these baselines only adopt one learning strategy (e.g., DOMINANT solely uses reconstruction and CoLA considers contrasting only), which results in a sub-optimal solution to anomaly detection. In contrast, SL-GAD jointly leverages two self-supervised learning strategies (generative and contrastive), which takes advantage of each other to acquire a higher performance.
- Our method obtains more considerable performance gains on detecting anomalies in citation networks (ACM, Cora, CiteSeer, and Pubmed) compared to which in social networks (BlogCatalog and Flickr). We observe that these social networks have a more significant degree (mean degree = 32.35) than citation networks (mean degree = 2.51), which may lead to an information loss when sampling subgraph views with a fixed size. We leave the efficient view sampling strategy for high-degree graphs as our future work.

5.4 Effectiveness of Components

We investigate the impact of different components of our method in this experiment. We first consider two variants

TABLE 3

Anomaly detection performance (i.e., AUC values) on six benchmark datasets. The best performance on each dataset is in bold.

Method	BlogCatalog	Flickr	ACM	Cora	CiteSeer	PubMed
AMEN [3]	0.6392	0.6573	0.5626	0.6266	0.6154	0.7713
Radar [4]	0.7401	0.7399	0.7247	0.6587	0.6709	0.6233
ANOMALOUS [5]	0.7237	0.7434	0.7038	0.5770	0.6307	0.7316
DOMINANT [6]	0.7468	0.7442	0.7601	0.8155	0.8251	0.8081
DGI [52]	0.5827	0.6237	0.6240	0.7511	0.8293	0.6962
CoLA [15]	0.7854	0.7513	0.8237	0.8779	0.8968	0.9512
SL-GAD	0.8184	0.7966	0.8538	0.9130	0.9136	0.9672

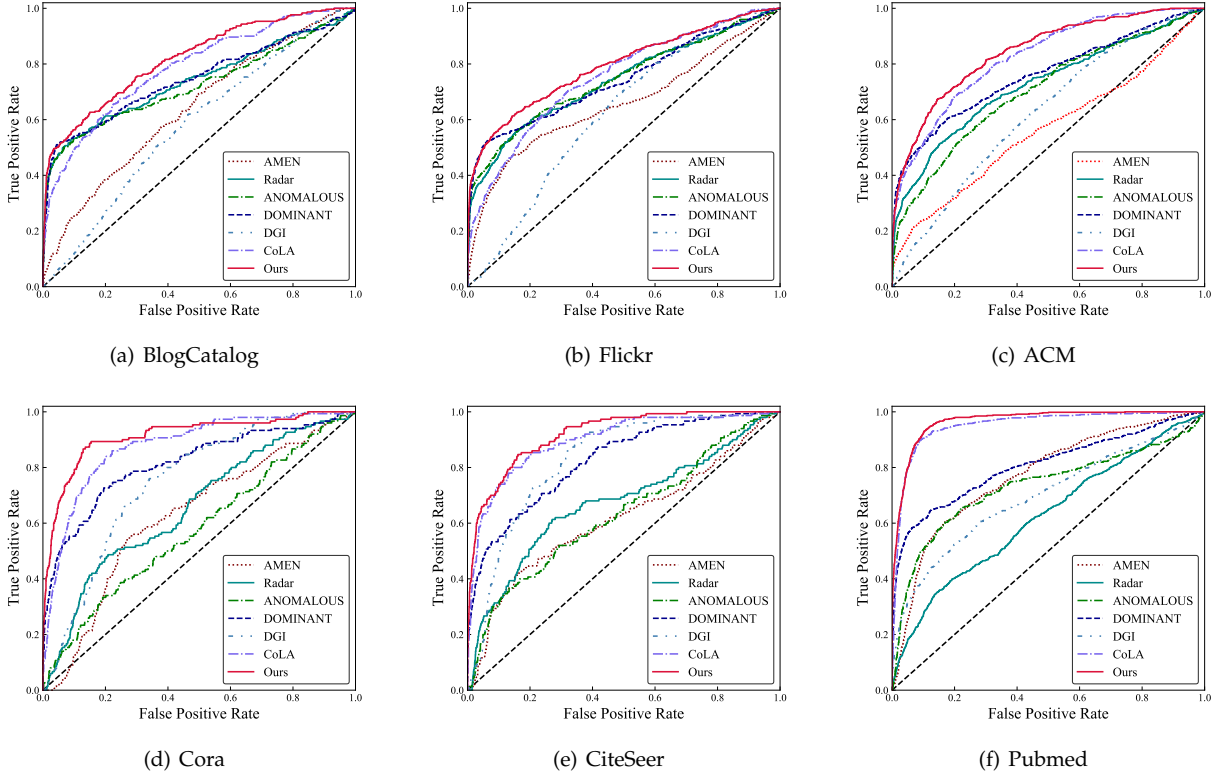


Fig. 3. ROC curves on six benchmark datasets. The larger the area under the curve, the better the performance of graph anomaly detection. "Ours" in the figure legends denotes the proposed method SL-GAD.

of SL-GAD, where SL-GAD-Con only uses contrastive self-supervised learning to identify anomalous nodes but excludes the generative term, and SL-GAD-Gen solely considers feature reconstruction to detect anomalies while the contrastive term is removed from the training loss and anomaly score. To study the effectiveness of designed anomaly scoring functions, we further construct SL-GAD-Unscaled and SL-GAD-Unweighted, where the first variant removes scalers in Equation (16) and (17), and the second variant sums generative and contrastive anomaly scores in an unweighted manner, i.e., $\alpha = \beta = 1$ in Equation (18). We report the results in Table 4 with the following observations:

- The best performance is achieved by the full SL-GAD, which validates the effectiveness of combining contrastive and generative self-supervised learning in a joint learning manner for graph anomaly detection. It also proves that the two self-supervised learning

strategies can mutually benefit each other in our method since each of them can recognize exclusive anomaly patterns in graphs.

- In all six datasets, SL-GAD-Con consistently outperforms SL-GAD-Gen, which demonstrates that contrastive self-supervised learning plays a more critical role in detecting anomalies than generative self-supervised learning. A possible reason is that the agreement between a target node and its neighbouring substructure is highly related to the graph anomalies, which is suggested in [15]. Compared to the results in Table 3, both variants can achieve a competitive performance to most baseline methods.
- Both anomaly score scaling and weighting facilitate graph anomaly detection on six datasets. When score scaling is disabled, adding generative and contrastive anomaly scores is likely to distort the final measurement because they are formed by different

TABLE 4

The results of ablation study to investigate the effectiveness of each component on SL-GAD. Specifically, we use SL-GAD-Con, SL-GAD-Gen, SL-GAD-Unweighted, and SL-GAD-Unscaled to denote SL-GAD without the generative module, contrastive module, anomaly score weighting, and anomaly score scaling, respectively.

Method	BlogCatalog	Flickr	ACM	Cora	CiteSeer	PubMed
SL-GAD	0.8184	0.7966	0.8538	0.9130	0.9136	0.9672
SL-GAD-Con	0.7899	0.7540	0.8308	0.8885	0.8830	0.9482
SL-GAD-Gen	0.7466	0.7442	0.7184	0.8143	0.7841	0.7982
SL-GAD-Unweighted	0.8069	0.7951	0.7972	0.9042	0.8908	0.9419
SL-GAD-Unscaled	0.7913	0.7812	0.8519	0.8924	0.8670	0.9632

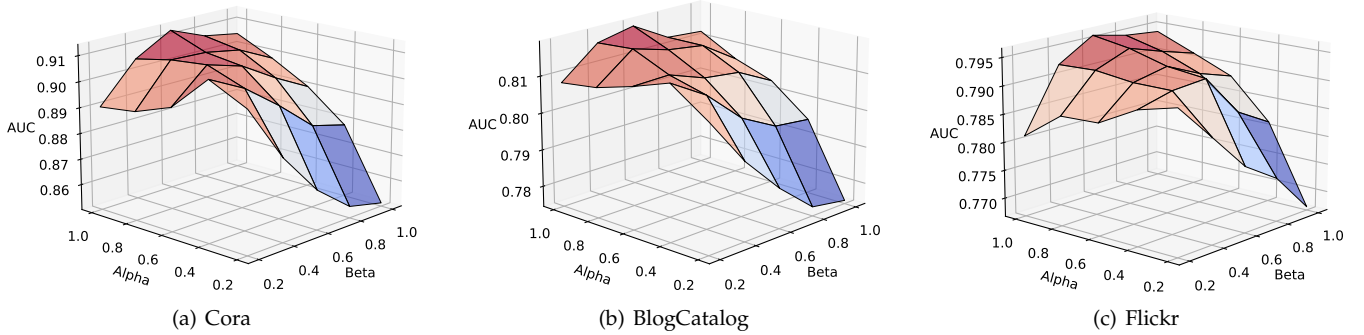


Fig. 4. AUC values of SL-GAD on Cora, BlogCatalog, and Flickr with different weights Alpha and Beta. A warmer color denotes a higher AUC value.

metrics and in different scales. On the other hand, removing score weights also hurts performance. A possible reason is that letting $\alpha = \beta = 1$ in Equation (18) causes inconsistencies between training and inference because: (1). the calculation of two types of anomaly score relies on trained graph encoder, generative decoder, and contrastive discriminators; (2). α and β are not equal to 1 during the training.

5.5 Parameters Sensitivity

In this subsection, we carry out a series of experiments to study the effectiveness of various hyper-parameters in SL-GAD, including the factors α and β to balance generative and contrastive terms, the evaluation rounds R , the sub-graph size K in graph view sampling, and the dimension of embedding D' .

5.5.1 Balance Factors

In this experiment, we discuss the impact of the balance factors α and β in Eq. (18) and (19). We respectively tune the two factors in a range of $\{0.2, 0.4, 0.6, 0.8\}$, and the results are illustrated in Figure 4. Due to limited space, we only show the results on Cora, BlogCatalog and Flickr datasets. According to the results, the AUC values show an upward trend with the increase of α , except when β is extremely small. Such observation demonstrates that contrastive self-supervised learning is dominant in anomaly detection performance compared with generative self-supervised learning. Furthermore, the selection of β highly depends on the specific dataset. For instance, Flickr needs a larger value ($\beta \geq 0.6$) while BlogCatalog prefers a small one ($\beta \leq 0.6$). The results show that it is necessary to find a trade-off between contrastive and generative terms according to the

properties of datasets. In practice, we fix $\alpha = 1$ and fine-tune the value of β for each dataset.

5.5.2 Evaluation Rounds

We investigate the effectiveness of evaluation rounds R in the inference stage of SL-GAD. The value of R is selected from $\{1, 5, 10, 20, 40, 80, 160, 320\}$. The visualized results are shown in Figure 5(a). It can be observed that the performance is poor when the evaluation rounds are insufficient. With larger R , the AUC values rise steadily within a certain range ($R \leq 80$), which indicates that a sufficient number of rounds is essential to prevent the bias caused by randomly sampling. However, when R is large enough ($R \geq 160$), AUC does not have a significant increasing trend even if R is doubled. Consequently, we keep R to be 160 to acquire a stable performance as well as an acceptable running speed.

5.5.3 Subgraph Size

We further explore the sensitivity of subgraph size K in graph view sampling. We run SL-GAD on six datasets for $K = \{1, 2, 4, 6, 8, 10, 12, 14\}$ and test the anomaly detection performance. The results are reported in Figure 5(b). As we can see from the figure, the performance of SL-GAD increases sharply with the growth of K when K is small and rapidly reaches the peak values. The peak values of AUC appear when $K = 2$ for some datasets and $K = 4$ for others. After the peak values, the performance drops with the increase of subgraph size. The results show that an appreciated subgraph size is needed to ensure a reliable detection performance. When K is extremely small, the model is hard to acquire sufficient neighboring information to detect anomalies; on the other hand, when K is too large, superfluous information would be included by the subgraph, which hurts the performance.

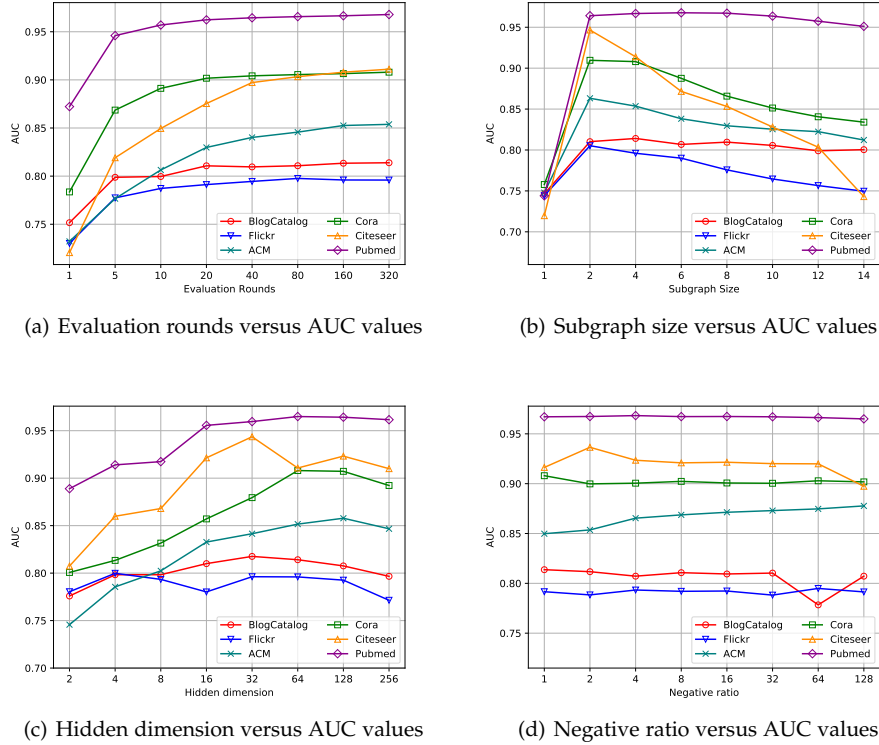


Fig. 5. The parameter sensitivity study of SL-GAD on six benchmark datasets. The subfigure (a) shows the performance of our method on different evaluation rounds, where other hyper-parameters are fixed to the default setting as discussed in Section 5.2. Similarly, subfigure (b), (c), and (d) studies the impact of subgraph size, hidden dimension, and negative ratio, respectively.

5.5.4 Embedding Dimension

In this experiment, we study the impact of the dimension D' of latent embedding in our GNN-based encoder. The results of varying the values of D' from 2 to 256 on six datasets are demonstrated in Figure 5(c). We can observe that in most datasets, the performance improves following the increase of hidden dimension when $D' \leq 32$. When D' is larger, there is a peak value of AUC for each dataset, and then the performance drops slightly. The decrease stems from the over-fitting problem due to the explosive parameter number. We summarize that D' should be in an appropriate range, e.g., from 32 to 128, and finally select 64 as a general value for all datasets.

5.5.5 Negative Ratio

In this experiment, we change the negative ratio from 1 to 128 to investigate the impact of contrastive negative samples on detection performance. The results are summarized in Figure 5(d), where we define the rate of negatives to positives as the negative ratio, and we have one positive and one negative sample by default in SL-GAD. In general, we observe that increasing the number of negative samples will not significantly affect the detection performance on most of the datasets (e.g., Cora, PubMed, BlogCatalog, and Flickr). A possible reason is that the devised multi-round evaluation mechanism is sufficient for SL-GAD to capture diverse contextual information without relying on a large number of negative samples. On the other hand, unlike other parameter studies, there does not exist a uniform

trend regarding the impacts of contrastive negatives on our method, e.g., we found that increasing negatives hurts detection performance on Cora and CiteSeer, but doing so will improve the performance on ACM.

6 CONCLUSION

In this paper, we studied the problem of unsupervised graph anomaly detection. We argued that existing approaches did not fully exploit the contextual information of a target node and count heavily on available supervision signals for graph anomaly detection. We proposed a novel self-supervised approach, SL-GAD, for graph anomaly detection. Our method first generates two different subgraph views of a target node as its contextual information. Then, we employ two key components, namely generative attribute reconstruction and multi-view contrastive learning, to fulfill this task. The attribute reconstruction leverages a generative learning schema, which identifies nodes differing from their neighbors in the attribute space, while the multi-view contrasting tells the difference between nodes and surrounding contexts directly in the hidden and structure space. Experimental results on six datasets demonstrate the superb performance of the proposed algorithm.

The proposed method is manually designed for anomaly detection. In the future, we will incorporate neural architecture search approaches [53], [54], [55] to automatically design models for anomaly detection.

REFERENCES

- [1] T. Pourhabibi, K.-L. Ong, B. H. Kam, and Y. L. Boo, "Fraud detection: A systematic literature review of graph-based anomaly detection approaches," *Decision Support Systems*, vol. 133, p. 113303, 2020.
- [2] M. Latah, "Detection of malicious social bots: A survey and a refined taxonomy," *Expert Systems with Applications*, vol. 151, p. 113383, 2020.
- [3] B. Perozzi and L. Akoglu, "Scalable anomaly ranking of attributed neighborhoods," in *Proceedings of the 2016 SIAM International Conference on Data Mining*. SIAM, 2016, pp. 207–215.
- [4] J. Li, H. Dani, X. Hu, and H. Liu, "Radar: Residual analysis for anomaly detection in attributed networks." in *International Joint Conferences on Artificial Intelligence*, 2017, pp. 2152–2158.
- [5] Z. Peng, M. Luo, J. Li, H. Liu, and Q. Zheng, "Anomalous: A joint modeling approach for anomaly detection on attributed networks." in *International Joint Conferences on Artificial Intelligence*, 2018, pp. 3513–3519.
- [6] K. Ding, J. Li, R. Bhanushali, and H. Liu, "Deep anomaly detection on attributed networks," in *Proceedings of the 2019 SIAM International Conference on Data Mining*. SIAM, 2019, pp. 594–602.
- [7] Y. Li, X. Huang, J. Li, M. Du, and N. Zou, "Specac: Spectral autoencoder for anomaly detection in attributed networks," in *Proceedings of the 28th ACM International Conference on Information and Knowledge Management*, 2019, pp. 2233–2236.
- [8] K. Ding, J. Li, N. Agarwal, and H. Liu, "Inductive anomaly detection on attributed networks," in *29th International Joint Conference on Artificial Intelligence*. International Joint Conferences on Artificial Intelligence, 2020, pp. 1288–1294.
- [9] V. Chandola, A. Banerjee, and V. Kumar, "Anomaly detection: A survey," *ACM computing surveys (CSUR)*, vol. 41, no. 3, pp. 1–58, 2009.
- [10] G. Pang, C. Shen, L. Cao, and A. v. d. Hengel, "Deep learning for anomaly detection: A review," *arXiv preprint arXiv:2007.02500*, 2020.
- [11] M. M. Breunig, H.-P. Kriegel, R. T. Ng, and J. Sander, "Lof: Identifying density-based local outliers," in *Proceedings of the 2000 ACM SIGMOD international conference on Management of data*, 2000, pp. 93–104.
- [12] B. Schölkopf, J. C. Platt, J. Shawe-Taylor, A. J. Smola, and R. C. Williamson, "Estimating the support of a high-dimensional distribution," *Neural computation*, vol. 13, no. 7, pp. 1443–1471, 2001.
- [13] D. Hendrycks, M. Mazeika, and T. Dietterich, "Deep anomaly detection with outlier exposure," *arXiv preprint arXiv:1812.04606*, 2018.
- [14] L. Ruff, R. A. Vandermeulen, N. Görnitz, A. Binder, E. Müller, K.-R. Müller, and M. Kloft, "Deep semi-supervised anomaly detection," *arXiv preprint arXiv:1906.02694*, 2019.
- [15] Y. Liu, Z. Li, S. Pan, C. Gong, C. Zhou, and G. Karypis, "Anomaly detection on attributed networks via contrastive self-supervised learning," *IEEE transactions on neural networks and learning systems*, 2021.
- [16] X. Liu, F. Zhang, Z. Hou, Z. Wang, L. Mian, J. Zhang, and J. Tang, "Self-supervised learning: Generative or contrastive," 2020.
- [17] L. Jing and Y. Tian, "Self-supervised visual feature learning with deep neural networks: A survey," *IEEE Transactions on Pattern Analysis and Machine Intelligence*, 2020.
- [18] Y. Liu, S. Pan, M. Jin, C. Zhou, F. Xia, and P. S. Yu, "Graph self-supervised learning: A survey," *arXiv preprint arXiv:2103.00111*, 2021.
- [19] P. Velickovic, W. Fedus, W. L. Hamilton, P. Liò, Y. Bengio, and R. D. Hjelm, "Deep graph infomax." in *International Conference on Learning Representations*, 2019.
- [20] K. Hassani and A. H. Khasahmadi, "Contrastive multi-view representation learning on graphs," in *International Conference on Machine Learning*. PMLR, 2020, pp. 4116–4126.
- [21] S. Wan, S. Pan, J. Yang, and C. Gong, "Contrastive and generative graph convolutional networks for graph-based semi-supervised learning," in *Proceedings of the AAAI Conference on Artificial Intelligence*, vol. 35, no. 11, 2021, pp. 10 049–10 057.
- [22] M. Jin, Y. Zheng, Y.-F. Li, C. Gong, C. Zhou, and S. Pan, "Multi-scale contrastive siamese networks for self-supervised graph representation learning," in *International Joint Conference on Artificial Intelligence*, 2021.
- [23] Y. You, T. Chen, Y. Shen, and Z. Wang, "Graph contrastive learning automated," in *International Conference on Machine Learning*, 2021.
- [24] Z. Wu, S. Pan, F. Chen, G. Long, C. Zhang, and P. S. Yu, "A comprehensive survey on graph neural networks," *IEEE Transactions on Neural Networks and Learning Systems*, pp. 1–21, 2020.
- [25] T. N. Kipf and M. Welling, "Semi-supervised classification with graph convolutional networks," in *International Conference on Learning Representations*, 2017.
- [26] P. Veličković, G. Cucurull, A. Casanova, A. Romero, P. Liò, and Y. Bengio, "Graph attention networks," in *International Conference on Learning Representations*, 2018.
- [27] W. Hamilton, Z. Ying, and J. Leskovec, "Inductive representation learning on large graphs," in *Advances in neural information processing systems*, 2017, pp. 1024–1034.
- [28] F. Frasca, E. Rossi, D. Eynard, B. Chamberlain, M. Bronstein, and F. Monti, "Sign: Scalable inception graph neural networks," in *ICML 2020 Workshop on Graph Representation Learning and Beyond*, 2020.
- [29] S. Geisler, D. Zügner, and S. Günnemann, "Reliable graph neural networks via robust aggregation," in *Advances in Neural Information Processing Systems*, 2020.
- [30] H. Wang, C. Zhou, X. Chen, J. Wu, S. Pan, and J. Wang, "Graph stochastic neural networks for semi-supervised learning," in *Advances in Neural Information Processing Systems*, 2020.
- [31] S. Zhu, S. Pan, C. Zhou, J. Wu, Y. Cao, and B. Wang, "Graph geometry interaction learning," in *Advances in Neural Information Processing Systems*, 2020.
- [32] M. Wu, S. Pan, L. Du, and X. Zhu, "Learning graph neural networks with positive and unlabeled nodes," *ACM Trans. Knowl. Discov. Data*, vol. 15, no. 6, Jun. 2021.
- [33] S. Zhu, C. Zhou, S. Pan, X. Zhu, and B. Wang, "Relation structure-aware heterogeneous graph neural network," in *2019 IEEE International Conference on Data Mining*. IEEE, 2019, pp. 1534–1539.
- [34] Z. Wu, S. Pan, G. Long, J. Jiang, X. Chang, and C. Zhang, "Connecting the dots: Multivariate time series forecasting with graph neural networks," in *Proceedings of the 26th ACM SIGKDD International Conference on Knowledge Discovery & Data Mining*, 2020, pp. 753–763.
- [35] D. Jin, Z. Yu, P. Jiao, S. Pan, P. S. Yu, and W. Zhang, "A survey of community detection approaches: From statistical modeling to deep learning," *arXiv preprint arXiv:2101.01669*, 2021.
- [36] S. Wan, C. Gong, P. Zhong, S. Pan, G. Li, and J. Yang, "Hyperspectral image classification with context-aware dynamic graph convolutional network," *IEEE Transactions on Geoscience and Remote Sensing*, 2020.
- [37] T. N. Kipf and M. Welling, "Variational graph auto-encoders," *arXiv preprint arXiv:1611.07308*, 2016.
- [38] P. Veličković, W. Fedus, W. L. Hamilton, P. Liò, Y. Bengio, and R. D. Hjelm, "Deep graph infomax," in *International Conference on Learning Representations*, 2018.
- [39] W. Hu, B. Liu, J. Gomes, M. Zitnik, P. Liang, V. Pande, and J. Leskovec, "Strategies for pre-training graph neural networks," in *International Conference on Learning Representations*, 2020.
- [40] Y. You, T. Chen, Z. Wang, and Y. Shen, "When does self-supervision help graph convolutional networks?" in *International Conference on Machine Learning*. PMLR, 2020, pp. 10 871–10 880.
- [41] Y. Jiao, Y. Xiong, J. Zhang, Y. Zhang, T. Zhang, and Y. Zhu, "Sub-graph contrast for scalable self-supervised graph representation learning," in *International Conference on Data Mining*, 2020.
- [42] Y. Tian, D. Krishnan, and P. Isola, "Contrastive multiview coding," in *Computer Vision—ECCV 2020: 16th European Conference, Glasgow, UK, August 23–28, 2020, Proceedings, Part XI 16*. Springer, 2020, pp. 776–794.
- [43] C. Tosh, A. Krishnamurthy, and D. Hsu, "Contrastive learning, multi-view redundancy, and linear models," in *Algorithmic Learning Theory*. PMLR, 2021, pp. 1179–1206.
- [44] H. Tong, C. Faloutsos, and J.-Y. Pan, "Fast random walk with restart and its applications," in *International Conference on Data Mining*. IEEE, 2006, pp. 613–622.
- [45] J. Klicpera, S. Weissenberger, and S. Günnemann, "Diffusion improves graph learning," in *Advances in Neural Information Processing Systems*, 2019, pp. 13 354–13 366.
- [46] Y. You, T. Chen, Y. Sui, T. Chen, Z. Wang, and Y. Shen, "Graph contrastive learning with augmentations," in *Advances in Neural Information Processing Systems*, 2020.
- [47] C. Zhou and R. C. Paffenroth, "Anomaly detection with robust deep autoencoders," in *Proceedings of the 23rd ACM SIGKDD international conference on knowledge discovery and data mining*, 2017, pp. 665–674.

- [48] Z. Ying, J. You, C. Morris, X. Ren, W. Hamilton, and J. Leskovec, "Hierarchical graph representation learning with differentiable pooling," in *Advances in neural information processing systems*, 2018, pp. 4800–4810.
- [49] L. Tang and H. Liu, "Relational learning via latent social dimensions," in *Proceedings of the 15th ACM SIGKDD international conference on Knowledge discovery and data mining*, 2009, pp. 817–826.
- [50] J. Tang, J. Zhang, L. Yao, J. Li, L. Zhang, and Z. Su, "Arnetminer: extraction and mining of academic social networks," in *Proceedings of the 14th ACM SIGKDD international conference on Knowledge discovery and data mining*, 2008, pp. 990–998.
- [51] P. Sen, G. Namata, M. Bilgic, L. Getoor, B. Galligher, and T. Eliassi-Rad, "Collective classification in network data," *AI magazine*, vol. 29, no. 3, pp. 93–93, 2008.
- [52] P. Veličković, W. Fedus, W. L. Hamilton, P. Liò, Y. Bengio, and R. D. Hjelm, "Deep graph infomax," in *International Conference on Learning Representations*, 2019.
- [53] M. Zhang, H. Li, S. Pan, X. Chang, C. Zhou, Z. Ge, and S. W. Su, "One-shot neural architecture search: Maximising diversity to overcome catastrophic forgetting," *IEEE Transactions on Pattern Analysis and Machine Intelligence*, 2020.
- [54] M. Zhang, H. Li, S. Pan, X. Chang, Z. Ge, and S. W. Su, "Differentiable neural architecture search in equivalent space with exploration enhancement," in *Advances in Neural Information Processing Systems*, 2020.
- [55] M. Zhang, H. Li, S. Pan, X. Chang, and S. Su, "Overcoming multi-model forgetting in one-shot nas with diversity maximization," in *Proceedings of the IEEE/CVF Conference on Computer Vision and Pattern Recognition*, 2020, pp. 7809–7818.